Gain-saturated 10.9 nm tabletop laser operating at 1 Hz repetition rate

D. Alessi,[1,2,*] D. H. Martz,[1,2] Y. Wang,[1,2] M. Berrill,[1,2] B. M. Luther,[1,2] and J. J. Rocca[1,2,3]

[1]*National Science Foundation Engineering Research Center for Extreme Ultraviolet Science and Technology, Colorado State University, Fort Collins 80523, Colorado, USA*

[2]*Electrical and Computer Engineering Department, Colorado State University, Fort Collins 80523, Colorado, USA*

[3]*Physics Department, Colorado State University, Fort Collins 80523, Colorado, USA*

**Corresponding author: dalessi@engr.colostate.edu*

Received November 24, 2009; accepted December 9, 2009;
posted January 7, 2010 (Doc. ID 120432); published January 29, 2010

We report the demonstration of a gain-saturated 10.9 nm tabletop soft x-ray laser operating at 1 Hz repetition rate. Lasing occurs by collisional electron impact excitation in the $4d\ ^1S_0 \rightarrow 4p\ ^1P_1$ transition of nickel-like Te in a line-focus plasma heated by a chirped-pulse-amplification Ti:sapphire laser. With an average power of 1 μW and pulse energy up to $\sim$2 μJ, this laser extends the ability to conduct tabletop laser experiments to a shorter wavelength. © 2010 Optical Society of America

OCIS codes: 140.7240, 340.7480.

There is great interest in extending tabletop soft x-ray lasers to shorter wavelengths for applications. Of particular interest is the development of gain-saturated lasers that can be fired repetitively, producing the average power required for many applications. Both capillary discharges and laser-created plasmas have been successfully used to demonstrate gain-saturated collisionally excited tabletop lasers that operate at wavelengths between 46.9 and 13.2 nm at repetition rates of several hertz [1–10]. However, the steep wavelength scaling of the energy necessary to pump such lasers imposes a challenge to the demonstration of gain-saturated high-repetition-rate lasers at shorter wavelengths. As a result, the use of tabletop soft x-ray lasers in applications has been limited to wavelengths above 13 nm. The shortest wavelength tabletop laser used in applications is a gain-saturated 13.2 nm nickel-like Cd laser that enabled the implementation of broad area microscopes with spatial resolution down to 38 nm [11].

Herein we report the demonstration of a gain-saturated tabletop 10.9 nm laser in the $4d\ ^1S_0 \rightarrow 4p\ ^1P_1$ transition of nickel-like Te that operates at 1 Hz repetition rate. Lasing in nickel-like Te was first demonstrated using 520 J of laser pump energy to heat a collisionally pumped plasma [12]. More recently gain in this transition was obtained in a tabletop setup using 1 J pulses of 8 ps duration impinging at a grazing angle of 23 deg to heat a precreated plasma [4]. However, the output laser intensity was weak and far from saturation, producing an insufficient photon flux for applications. Model computations conducted using a 1.5 dimension hydrodynamic/atomic physics code developed in-house suggest that gain-saturated lasing in the $\lambda = 10.9$ nm $4d\ ^1S_0 \rightarrow 4p\ ^1P_1$ transition of nickel-like Te can be generated by irradiation of a solid Te target with a sequence of pulses from a chirped pulse amplification laser with a total energy of less than 4 J. Figure 1 shows the simulated evolution of the plasma parameters and resulting gain coefficient for the 10.9 nm laser line. The plasma is assumed to be created by a sequence of two 210 ps duration prepulses with intensities of 4.8×10^{10} W cm^{-2} and 1.8×10^{12} W cm^{-2} separated by 5.6 ns, and to be subsequently transiently heated with a 5 ps FWHM duration pulse with an intensity of 9.8×10^{13} W cm^{-2} impinging at 30 deg grazing incidence. This pumping geometry, which is inherently a traveling wave, takes advantage of the refraction of the pump beam in the electron density gradient of the precreated plasma to efficiently deposit energy into a plasma density region with optimum conditions for amplification [3–6,8–10,13]. The first laser pulse is responsible for creating the ion density profile, and the second laser pulse heats the plasma, ionizing 40% of the ions into the nickel-like state over a relatively broad region [Fig. 1(c)]. A dip in the degree of ionization develops between the outer region where the prepulse energy is absorbed and the target region dominated by pres-

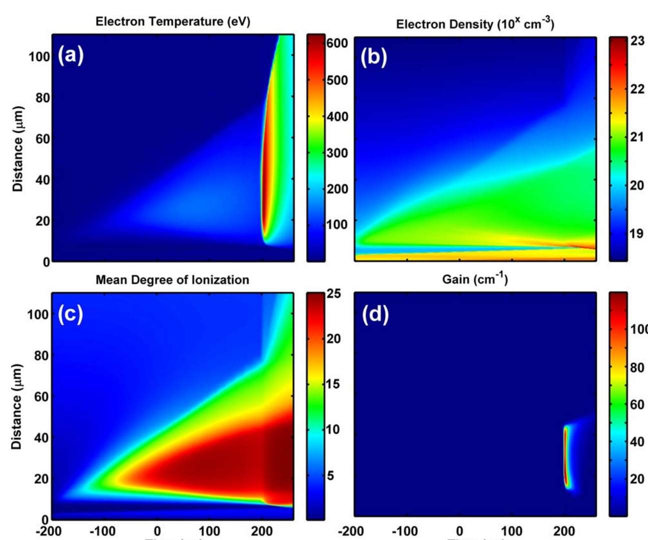

Fig. 1. (Color online) Simulated evolution of (a) electron temperature, (b) electron density, (c) mean degree of ionization, and (d) $\lambda = 10.9$ nm gain coefficient for a Te plasma amplifier.

0146-9592/10/030414-3/$15.00

sure ionization. The short pulse energy is coupled by refraction into a region where the electron density is $\sim 4 \times 10^{20}$ cm^{-3} and rapidly increases the electron temperature to ~600 eV [Fig. 1(a)]. This is computed to generate a transient inversion resulting in a peak gain of ~120 cm^{-1} with a FWHM duration of ~9 ps [Fig. 1(d)]. A 3-D post-processor ray-tracing code predicts a spatially integrated gain of 64 cm^{-1}. The experiments described below used similar excitation conditions to demonstrate a $\lambda = 10.9$ nm tabletop nickel-like Te laser operating at a repetition rate of 1 Hz with an average power of ~1 μW.

The experiment was conducted by rapidly heating a 5-mm-wide solid Te slab target at the irradiation conditions described above using a chirped-pulse-amplification Ti:sapphire laser system. Three stages of amplification were used to amplify $\lambda = 800$ nm pulses to energies up to 5.5 J before compression. After the third amplification stage the stretched pulses have a duration of 210 ps. A beam splitter placed after the final amplification stage was used to redirect 40% of the energy into a prepulse arm used to create a plasma with relatively smooth density gradients. About 2% of the energy was split to create an initial plasma that was subsequently ionized to the nickel-like ionization stage by the second 210 ps duration pulse. The two prepulses, separated by 5.6 ns, were focused into a 30 μm $\times$ 5 mm FWHM line onto the target. The remaining 60% of the laser energy was compressed into a 5 ps FWHM pulse in a vacuum grating compressor constructed using dielectric diffraction gratings [14] and focused into an overlapping line of the same dimension. The plasma emission was filtered by a 0.3-μm-thick Al foil and a 0.3-μm-thick Zr foil both with parylene support and was directed onto a grazing incidence spectrometer consisting of a 1200 lines/mm variable-line-spaced grating and a backilluminated CCD detector.

Figure 2 shows the measured $\lambda = 10.9$ nm laser intensity as a function of time delay between the peaks of the main prepulse and the short pulse. Strong soft x-ray lasing was observed to take place over a relatively narrow range of excitation delays centered at 200 ps. Lasing is observed to cease when the delay is increased to 400 ps. However, further increase of the delay results in weak lasing around 550 ps. This late laser pulse was predicted by the simulations. It occurs when Co-like ions recombine into Ni-like ions, indicating that the plasma is slightly over-ionized at the time of peak laser gain.

Figure 3(a) shows a series of on-axis single-shot spectra and their corresponding vertical integrations for plasmas of different lengths between $L = 1.8$ and 5 mm. The total pump energy on the target was fixed at 3.4 J. For a target length of 1.8 mm the 10.9 nm laser line is very weak and has an intensity similar to that of other plasma lines. The soft x-ray laser intensity rapidly grows with target length to dominate the entire spectra, eventually reaching saturation. From these spectra it was determined that for the 5 mm target the soft x-ray laser beam divergence in the direction parallel to the target is 8.5 ± 1 mrad. The measured soft x-ray laser intensity as a function of target length is shown in Fig. 3(b). The line is a fit of the data with an equation by Tallents *et al.* [15] that takes into account gain saturation. The fit shows a small signal gain of $g_0 = 45.3$ cm^{-1} and an integrated

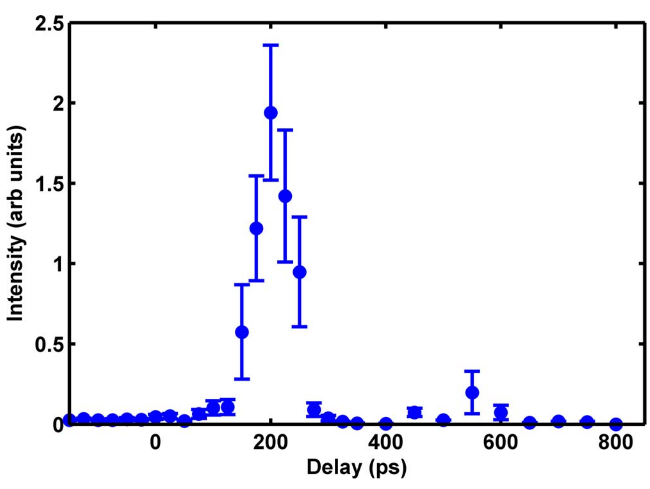

Fig. 2. (Color online) Measured $\lambda = 10.9$ nm laser intensity as a function of delay between the prepulse and short pulse.

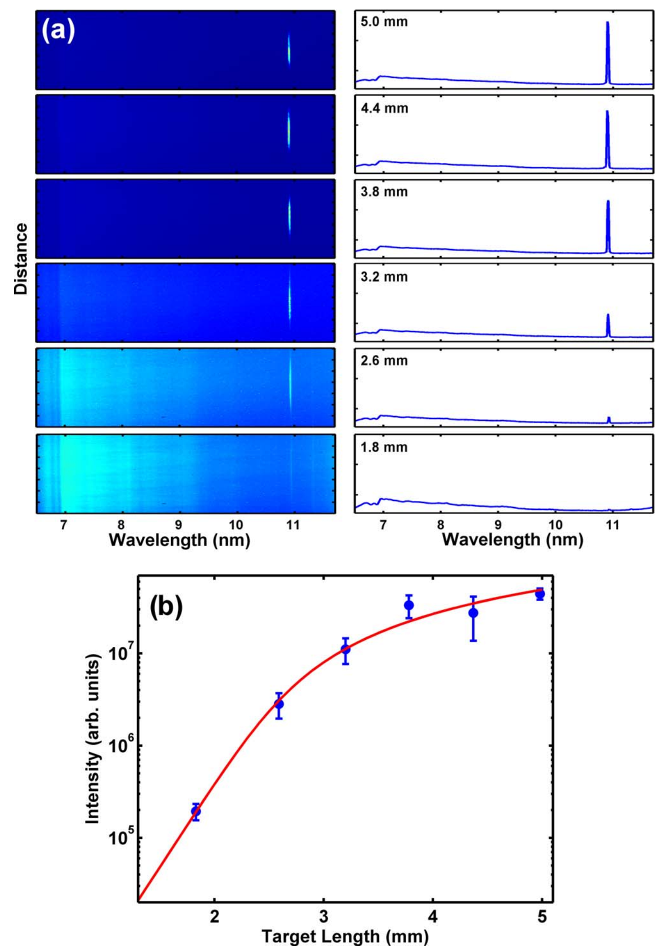

Fig. 3. (Color online) (a) On-axis single-shot spectra from the Te plasma for increasing plasma column lengths from 1.8 to 5 mm. Strong lasing is observed at 10.9 nm. (b) Measured laser line intensity as a function of plasma column length. Each data point is an average of eight laser shots, and error bars correspond to one standard deviation.

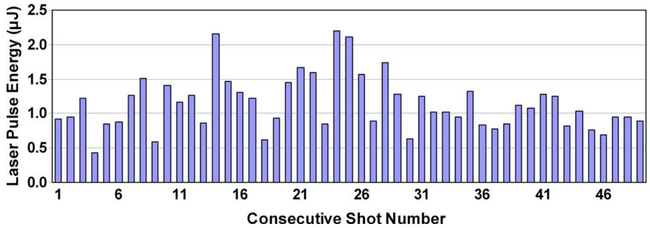

Fig. 4. (Color online) Sequence of $\lambda = 10.9$ nm laser shots acquired at 1 Hz repetition rate achieving an average power of ~ 1 μW.

gain length product of 14.1 at 5 mm. At about 3 mm, the intensity starts to show signs of saturation.

Results of the variation of the soft x-ray laser pulse energy at a laser repetition rate of 1 Hz are shown in Fig. 4. These data were obtained pumping a 6-mm-wide Te target with 4.2 J of total laser pump energy on target. The target was continually moved at a speed of 200 μm per second to renew the surface irradiated by each shot. The soft x-ray laser average power obtained was ~ 1 μW. The shot-to-shot energy variation is characterized by a standard deviation of 36%. This large variation can be explained by the brittle nature of the tellurium target, which often fractures locally near the edges when irradiated with the high-energy pulses used in this experiment, affecting the subsequent laser shot. In comparison, in a similar experiment conducted with a Ag target that does not fracture we measured a $\lambda = 13.9$ nm output pulse laser energy variation characterized by an 8% standard deviation. An increase in the speed at which the Te target is moved should decrease the shot-to-shot fluctuation in soft x-ray laser pulse energy. The energy of the most intense laser pulses was estimated to be ~ 2 μJ from the CCD counts, taking into account the attenuation of the filters, the grating efficiency, and the quantum efficiency of the detector. Assuming a laser pulse duration of 4–5 ps and a near-field laser spot of ~ 15 μm diameter, both resulting from the 3-D postprocessor ray-trace simulation, the laser beam intensity is estimated to reach $\sim 2.5 \times 10^{11}$ W cm^{-2}. This exceeds the $0.6 - 1.4 \times 10^{10}$ W/cm^2 computed saturation intensity of this line for the plasma conditions of the experiment.

In summary, we have extended gain-saturated tabletop soft x-ray lasers down to 10.9 nm by transient excitation of a nickel-like Te plasma. To our knowledge, this is the shortest wavelength gain-saturated tabletop laser reported to date. With an average power of ~ 1 μW and pulse energies of up to 2 μJ, this laser will enable applications of tabletop lasers at shorter wavelengths.

We thank Eric Gullikson for measuring the transmission of the aluminum and zirconium filters. This work was supported by the National Science Foundation (NSF) Engineering Research Center (ERC) for Extreme Ultraviolet Science and Technology NSF Award EEC-0310717 and by the Chemical Sciences, Geosciences and Biosciences Division, Office of Basic Energy Sciences, Office of Science, U.S. Department of Energy (DOE). M. B. acknowledges support from the Department of Energy (DOE) CSGF grant DE-FG02-97ER25308.

References

1. B. R. Benware, C. D. Macchietto, C. H. Moreno, and J. J. Rocca, Phys. Rev. Lett. **81**, 5804 (1998).
2. S. Sebban, R. Haroutunian, P. Balcou, G. Grillon, A. Rousse, S. Kazamias, T. Marin, J. P. Rousseau, L. Notebaert, M. Pittman, J. P. Chambaret, A. Antonetti, D. Hulin, D. Ros, A. Klisnick, A. Carillon, P. Jaegle, G. Jamelot, and J. F. Wyart, Phys. Rev. Lett. **86**, 3004 (2001).
3. B. M. Luther, Y. Wang, M. A. Larotonda, D. Alessi, M. Berrill, M. C. Marconi, J. J. Rocca, and V. N. Shlyaptsev, Opt. Lett. **30**, 165 (2005).
4. Y. Wang, M. A. Larotonda, B. M. Luther, D. Alessi, M. Berrill, V. N. Shlyaptsev, and J. J. Rocca, Phys. Rev. A **72**, 053807 (2005).
5. J. J. Rocca, Y. Wang, M. A. Larotonda, B. M. Luther, M. Berrill, and D. Alessi, Opt. Lett. **30**, 2581 (2005).
6. D. Alessi, B. M. Luther, Y. Wang, M. A. Larotonda, M. Berrill, and J. J. Rocca, Opt. Express **13**, 2093 (2005).
7. M.-C. Chou, P.-H. Lin, C.-A. Lin, J.-Y. Lin, J. Wang, and S.-Y. Chen, Phys. Rev. Lett. **99**, 063904 (2007).
8. K. Cassou, S. Kazamias, D. Ros, F. Plé, G. Jamelot, A. Klisnick, O. Lundh, F. Lindau, A. Persson, C.-G. Wahlström, S. de Rossi, D. Joyeux, B. Zielbauer, D. Ursescu, and T. Kühl, Opt. Lett. **32**, 139 (2007).
9. S. Kazamias, K. Cassou, D. Ros, F. Ple, G. Jamelot, A. Klisnick, O. Lundh, F. Lindau, A. Persson, C.-G. Wahlstrom, S. de Rossi, D. Joyeux, B. Zielbauer, D. Ursescu, and T. Kuhl, Phys. Rev. A **77**, 033812 (2008).
10. H. T. Kim, I. W. Choi, N. Hafz, J. H. Sung, T. J. Yu, K. H. Hong, T. M. Jeong, Y. C. Noh, D. K. Ko, K. A. Janulewicz, J. Tummler, P. V. Nickles, W. Sandner, and J. Lee, Phys. Rev. A **77**, 023807 (2008).
11. G. Vaschenko, C. Brewer, F. Brizuela, Y. Wang, M. A. Larotonda, B. M. Luther, M. C. Marconi, J. J. Rocca, and C. S. Menoni, Opt. Lett. **31**, 1214 (2006).
12. H. Daido, S. Ninomiya, T. Imani, R. Kodama, M. Takagi, Y. Kato, K. Murai, J. Zhang, Y. You, and Y. Gu, Opt. Lett. **21**, 958 (1996).
13. R. Keenan, J. Dunn, P. K. Patel, D. F. Price, R. F. Smith, and V. N. Shlyaptsev, Phys. Rev. Lett. **94**, 103901 (2005).
14. D. H. Martz, H. T. Nguyen, D. Patel, J. A. Britten, D. Alessi, E. Krous, Y. Wang, M. A. Larotonda, J. George, B. Knollenberg, B. M. Luther, J. J. Rocca, and C. S. Menoni, Opt. Express **17**, 23809 (2009).
15. G. J. Tallents, Y. Abou-Ali, M. Edwards, R. E. King, G. J. Pert, S. J. Pestehe, F. Strati, R. Keenan, C. L. S. Lewis, S. Topping, O. Guilbaud, A. Klisnick, D. Ros, R. Clarke, D. Neely, and M. Notley, in Eighth International Conference on X-ray Lasers, J. J. Rocca, J. Dunn, and S. Suckewer, eds., AIP Conference Proceedings Vol. C641 (AIP, 2002), p. 291.